0026-895X/08/7401-203–212$20.00
MOLECULAR PHARMACOLOGY
Copyright © 2008 The American Society for Pharmacology and Experimental Therapeutics
Mol Pharmacol 74:203–212, 2008

Vol. 74, No. 1
44891/3355431
Printed in U.S.A.

Individually Monitoring Ligand-Induced Changes in the Structure of the $GABA_A$ Receptor at Benzodiazepine Binding Site and Non–Binding-Site Interfaces

L. M. Sharkey and C. Czajkowski

Neuroscience Training Program (L.M.S., C.C.), and Department of Physiology (C.C.), University of Wisconsin–Madison, Madison, Wisconsin

Received January 3, 2008; accepted April 18, 2008

ABSTRACT

The mechanisms by which the GABA and benzodiazepine (BZD) binding sites of the GABA-A receptor are allosterically coupled remain elusive. In this study, we separately monitored ligand-induced structural changes in the BZD binding site (α/γ interface) and at aligned positions in the α/β interface. α_1His101 and surrounding residues were individually mutated to cysteine and expressed with wild-type $\beta2$ and $\gamma2$ subunits in *Xenopus laevis* oocytes. The accessibilities of introduced cysteines to modification by methanethiosulfonate ethylammonium (MTSEA)-Biotin were measured in the presence and absence of GABA-site agonists, antagonists, BZDs, and pentobarbital. The presence of flurazepam or the BZD-site antagonist flumazenil (Ro15-1788) decreased the rate of modification of α_1H101C at the BZD binding site. GABA and muscimol each increased MTSEA-Biotin modification of α_1H101C located at the BZD-site, gabazine (SR-95531, a GABA binding site antagonist) decreased the rate, whereas pentobarbital had no effect. Modification of α_1H101C at the α/β interface was significantly slower than modification of α_1H101C at the BZD site, and the presence of GABA or flurazepam had no effect on its accessibility, indicating the physicochemical environments of the α/γ and α/β interfaces are different. The data are consistent with the idea that GABA-binding site occupation by agonists causes a GABA binding cavity closure that is directly coupled to BZD binding cavity opening, and GABA-site antagonist binding causes a movement linked to BZD binding cavity closure. Pentobarbital binding/gating resulted in no observable movements in the BZD binding site near α_1H101C, indicating that structural mechanisms underlying allosteric coupling between the GABA and BZD binding sites are distinct.

Benzodiazepines (BZDs) are one of the most commonly prescribed classes of drugs in the United States and are used as anxiolytics, anticonvulsants, sleep aids, muscle relaxants, and antipsychotics (Doble and Martin, 1996; Hevers and Luddens, 1998; Rudolph et al., 2001; Rudolph and Mohler, 2004). BZDs exert their effects by binding to the GABA-A receptor and allosterically modulating GABA-activated currents. Although studies have shown that GABA and BZD binding cause reciprocal increases in the affinities of these ligands for their respective binding sites (Tallman et al., 1978; Karobath and Sperk, 1979; Choi et al., 1981; Olsen and Snowman, 1982; Hattori et al., 1986; Rogers et al., 1994), little is known about the structural mechanisms involved in coupling the two sites.

The GABA-A receptor mediates the majority of synaptic inhibition in the brain and is a member of the cys-loop family of receptors, which includes the nicotinic acetylcholine receptor (nAChR), the serotonin $5HT_3$ receptor, and the glycine receptor (Ortells and Lunt, 1995). Like other members of the cys-loop receptor family, the receptor consists of five subunits arranged around a central ion-conducting channel. The majority of native receptors are composed of two α_1 subunits, two β_2 subunits and one γ_2 subunit (McKernan and Whiting, 1996); each receptor contains two GABA binding sites located at the β/α subunit interfaces and one BZD binding site lo-

This work was supported by National Institutes of Health, National Institute of Neurological Disorders and Stroke grant NS34727 (to C.C.).

This work appears in the doctoral thesis of L.M.S.: *Structural Elements That Govern Benzodiazepine Modulation of the GABA-A Receptor*. Ph.D. thesis, University of Wisconsin–Madison, 2004. This work was previously presented in abstract form: Sharkey LM, Czajkowski C. Evidence that the two α_1 subunit interfaces (α/γ and α/β) of the $GABA_A$ receptor are structurally different and play different roles in receptor function. *Soc Neurosci Abstr* **28:**40.4.

Article, publication date, and citation information can be found at http://molpharm.aspetjournals.org.
doi:10.1124/mol.108.044891.

ABBREVIATIONS: BZD, benzodiazepine; MTSEA, methanethiosulfonate ethylammonium; nAChR, nicotinic acetylcholine receptor; BCCM, methyl betacarboline-3-carboxylate; FLZM, flurazepam; GABA-A, GABA type A; PENTO, pentobarbital; Ro15-4513, ethyl-8-azido-5,6-dihydro-5-methyl-6-oxo-4*H*-imidazo(1,5-α)(1,4)benzodiazepine-3-carboxylate; SR95531, gabazine (2-(3-carboxypropyl)-3-amino-6-(4 methoxyphenyl)pyridazinium bromide); Ro15-1788, flumazenil (8-fluoro-5,6-dihydro-5-methyl-6-oxo-4*H*-imidazo[1,5*a*][1,4]benzodiazepine-3-carboxylic acid, ethyl ester).

cated at the α/γ subunit interface (Fig. 1). A single α_1 subunit contributes to forming both a GABA and BZD binding site.

The BZD binding site is located on the extracellular surface of the GABA-A receptor and is formed by residues located in at least six noncontiguous regions at the α/γ interface, historically designated loops A to F (for review, see Sigel, 2002). The BZD recognition site binds a large selection of ligands, agonists that potentiate GABA induced current (positive modulators) (Macdonald and Barker, 1978), inverse agonists that inhibit GABA current (negative modulators) (Oakley and Jones, 1980; Macdonald et al., 1992), and antagonists that competitively bind at the BZD binding site but have no effect on GABA current (zero modulators) (Braestrup et al., 1982). Because the therapeutic value of BZDs depends upon their efficacy in modulating I_{GABA}, mapping structural rearrangements involved in mediating the full range of BZD actions from positive to negative modulation of I_{GABA} is essential.

Here, we used the substituted cysteine accessibility method to monitor movements within the BZD binding site near α_1His101. Site-directed mutagenesis, photolabeling studies, and molecular modeling have shown that α_1His101 resides within the core of the BZD binding site (Duncalfe et al., 1996; Dunn et al., 1999; Sieghart, 2006; Tan et al., 2007). α_1His101 and surrounding residues were individually mutated to cysteine. Changes in the ability of the sulfhydryl-specific reagent (MTSEA-Biotin) to modify the introduced cysteines were used to report structural movements that occur in the BZD binding site when GABA-site ligands as well as pentobarbital and BZDs bind. Any alteration in the modification rate of the introduced cysteine induced by these ligands indicates that a change in the local environment near that cysteine has occurred (i.e., movements). In this study, we demonstrated that GABA binding site occupation seemed sufficient for inducing movement in the BZD binding site near α_1His101 and that the structural mechanisms underlying coupling between the GABA and BZD binding sites were distinct from mechanisms involved in pentobarbital actions.

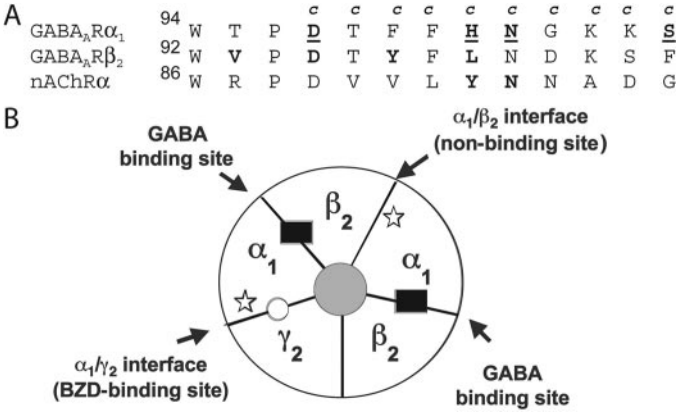

Fig. 1. A, alignment of "loop A" binding site regions from the GABA-A receptor rat α_1 and β_2 subunits and the nAChR torpedo α subunit. Residues in the GABA$_A$ receptor α_1 subunit that were mutated to cysteine are denoted by a "c" above the wild-type residue. Residues in α_1 identified in this study that are accessible to MTSEA-Biotin are underlined. Residues previously identified in the GABA-A receptor β_2 subunit and in the α subunit of the nAChR as being accessible to sulfhydryl-specific reagents are depicted in bold (Sullivan and Cohen, 2000; Boileau et al., 2002). B, schematic of a $\alpha_1\beta_2\gamma_2$ GABA$_A$ receptor. The GABA binding sites (β/α interfaces) are indicated by black rectangles and the BZD site (α/γ interface) by a white circle. Stars show the locations of the introduced cysteine mutations in the α_1 subunits. The mutations are located at the α/γ interface (BZD binding site) and at the α/β interface (nonbinding site).

Materials and Methods

Site-Directed Mutagenesis. Rat cDNA encoding α_1, β_2, and γ_{2S} receptor subunits in the pGH19 vector (Liman et al., 1992; Robertson et al., 1996) were used for all molecular cloning and functional studies. Cysteine mutations were introduced into pGH19 rat α_1 using recombinant polymerase chain reaction as described previously (Boileau et al., 1999; Kucken et al., 2000). Cysteine substitutions were introduced at positions Asp97, Thr98, Phe99, Phe100, His101, Asn102, Gly103, Lys104, Lys105, and Ser106. The mutant α_1 subunits are designated by the wild-type residue, residue number in the mature rat α_1 subunit followed by cysteine introduced (e.g., H101C). The presence of the mutations was verified using diagnostic endonuclease restriction digestion and double-stranded sequencing.

Expression in *Xenopus laevis* Oocytes. *X. laevis* oocytes were prepared as described previously (Boileau et al., 1998). Capped cRNA coding for the wild-type and mutant subunits was synthesized by in vitro transcription from NheI-linearized cDNA template using the mMessage mMachine T7 kit (Ambion, Austin, TX). GABA$_A$ receptor α_1 or α_1-mutant subunits were expressed with wild-type β_2 and γ_2 subunits by injection of 5 nl of cRNA (5–50 ng/μl/subunit) mixed in a ratio of 1:1:10 ($\alpha/\beta/\gamma$), dissolved in RNase-free water. Mean maximal responses to GABA were between 250 nA and 10 μA. Oocytes were stored at 16°C in ND96 medium (96 mM NaCl, 2 mM KCl, 1.8 mM $CaCl_2$, 1 mM $MgCl_2$, and 5 mM HEPES, pH 7.4) supplemented with 100 μg/ml gentamicin and 100 μg/ml BSA and were used for electrophysiological recording after 2 to 14 days.

Electrophysiological Recording. Oocytes under two-electrode voltage-clamp ($V_{hold} = -80$ mV) were perfused at a rate of 5 ml/min with ND96 recording solution. The bath volume was 200 μl. Electrodes were filled with 3 M KCl and had a resistance of 0.5 to 1.7 MΩ. Drugs and reagents were dissolved in ND96. The stock MTSEA-Biotin solution and BCCM were made in DMSO. Final concentration of DMSO in applied solutions was $\leq$1.0%. Standard two-electrode voltage clamp recording was performed using a GeneClamp 500 (Axon Instruments) interfaced to a computer with a Digidata 1200 (Molecular Devices, Sunnyvale, CA). Data acquisition and analysis were performed using pCLAMP 6 (Molecular Devices).

GABA EC_{50} Analysis. Concentration response experiments were performed as described previously (Boileau and Czajkowski, 1999). GABA responses were scaled for rundown or runup by comparison with a low, nondesensitizing concentration of drug applied just before the drug concentration tested. Concentrations were tested starting from lowest to highest and then reversing the order in the same oocyte. Concentration response curves for GABA were fit with the equation $I = I_{max} / (1 + (EC_{50}/[A])^{nH})$, where A is the agonist concentration, EC_{50} is the concentration of GABA eliciting half-maximal current amplitude, I_{max} is the maximal current amplitude, I is the current amplitude, and n_H is the Hill coefficient. Concentration response curves were plotted using Prism v.4.0 (GraphPad Software, San Diego, CA).

FLZM EC_{50} Analysis. Flurazepam (FLZM) potentiation was recorded at GABA EC_{13-17}. For each oocyte, we compared the current response of a low concentration test pulse of GABA to the current response of a 10 mM test pulse of GABA (peak current for all receptors) and, using a standard Hill equation, estimated EC_{50} for that oocyte to determine the appropriate GABA EC_{13-17} concentration to use when measuring BZD responses. FLZM potentiation is defined as (I-(GABA+FLZM)/I-GABA) $-$ 1, where I-(GABA+FLZM) is the current response in the presence of flurazepam and I-GABA is the control GABA current. FLZM concentrations were tested starting from lowest to highest. Concentration response curves for FLZM were fit with the equation $P = P_{max}/(1 + (EC_{50}/[A])^{nH})$, where A is the FLZM concentration, EC_{50} is the concentration of FLZM eliciting half-maximal current potentiation, P_{max} is the maximal FLZM po-

tentiation of I-GABA, P is the potentiation amplitude, and n_H is the Hill coefficient. Concentration response curves were plotted using Prism v.4.0 (GraphPad Software).

Pulse Protocol for Calculating MTSEA-Biotin Effects. The sulfhydryl-specific reagent used was MTSEA-Biotin, obtained from Toronto Research Chemicals (Toronto, ON, Canada). We use MTSEA-Biotin because it is impermeant to the membrane, it is not charged, its size (similar to that of BZDs) is suitable for fitting within the binding site, and it is bulky enough to make it likely that covalently attaching it to an introduced cysteine will result in a functional effect. Oocytes were stabilized before addition of MTSEA-Biotin by application of GABA and GABA+FLZM at 5-min intervals until the GABA-activated currents (I-GABA) and FLZM potentiation of I-GABA varied by <6%. GABA concentrations used were $EC_{13–17}$ and FLZM concentrations used were EC_{95} for each mutant. After the GABA and FLZM responses were stabilized, freshly diluted 2 mM MTSEA-Biotin was applied for 2 min, the cell was washed for 5 min, and then GABA and GABA+FLZM responses were measured. The effect of MTSEA-Biotin on GABA current was calculated as (I-GABApost/I-GABApre) − 1, where I-GABApost is the current elicited by GABA after MTS application, and I-GABApre is the current elicited by GABA before MTS application. The effect of MTSEA-Biotin on FLZM potentiation was calculated as ($FLZM_{post}$/$FLZM_{pre}$) − 1, where $FLZM_{pre}$ was the FLZM potentiation of I-GABA before MTS application and $FLZM_{post}$ was the FLZM potentiation of I-GABA after MTS application.

Rate of MTSEA-Biotin Modification. The rate of MTS reagent covalent modification of introduced cysteines was determined by measuring the effect of sequential applications of subsaturating concentrations of MTSEA-Biotin on I-GABA and FLZM potentiation of I-GABA. $EC_{13–17}$ GABA or $EC_{13–17}$ GABA followed by $EC_{13–17}$ GABA+EC_{95} FLZM was applied, and the cell was washed for 30 s. MTS reagent was applied for 5 to 20 s, the cell was washed for 2.5 min, and the procedure was repeated until changes in I-GABA and FLZM potentiation reached a plateau. Before the reaction rate was measured, GABA and GABA+FLZM were applied every 3 min until the response was stable to ± 6%. The effects of agonists and antagonists on the rate of MTS modification were tested by coapplying MTSEA-Biotin with GABA (EC_{95}), SR-95531 (IC_{95}), pentobarbital (500 μM), BCCM (EC_{95}), FLZM (EC_{95}), or Ro15-1788 (EC_{95}) for all mutants. The change in current was plotted versus cumulative time of MTS exposure. A pseudo–first-order rate constant was calculated from the change in I-GABA and FLZM potentiation. Peak values at each time point were normalized to the initial peak at time = 0 s, and a pseudo–first-order rate constant (k_1) was determined by fitting the data with a single exponential decay equation: $y = \text{span} \cdot e^{-kt} +$ plateau using Prism v.4.0 (GraphPad Software). Because the data are normalized to values at time 0, span = 1 − plateau. The second-order rate constant (k_2) for MTS reaction was determined by dividing the calculated pseudo–first-order rate constant by the concentration of MTSEA-Biotin used. To verify the accuracy of this protocol, second-order rate constants were determined using at least two different concentrations of MTSEA-Biotin for several mutants.

The drug concentrations used to modify α_1D97C$\beta_2\gamma_2$ receptors (monitoring changes in I-GABA) were as follows: control = 4 mM MTS; +FLZM = 4 mM MTS and 6 μM FLZM; +BCCM = 4 mM MTS and 1 μM BCCM; +GABA = 4 mM MTS and 2 mM GABA. The drug concentrations used to modify α_1H101Cβ_2 receptors (monitoring changes in I-GABA) were as follows: control = 1 mM MTS; +FLZM = 1 mM MTS and 100 μM FLZM; +Ro15-1788 = 1 mM MTS and 1 μM Ro15-1788; +GABA = 1 mM MTS and 300 μM GABA. The drug concentrations used to modify α_1H101C$\beta_2\gamma_2$ receptors (monitoring FLZM potentiation of I-GABA) were as follows: control = 50 μM MTS; +FLZM = 50 μM MTS and 100 μM FLZM; +Ro15-1788 = 50 μM MTS and 3 μM Ro15-1788; +GABA = 5 μM MTS and 1 mM GABA; +PENTO = 50 μM MTS and 500 μM PENTO; +Muscimol = 5 μM MTS and 300 μM Muscimol. The drug concentrations used to modify α_1H101C$\beta_2\gamma_2$ receptors (monitoring changes in I-GABA) were as follows: control = 1 mM MTS; +FLZM = 1 mM MTS and 100 μM FLZM; +Ro15-1788 = 100 μM MTS and 3 μM Ro15-1788; +GABA = 250 μM MTS and 2 mM GABA. The drug concentrations used to modify α_1N102C$\beta_2\gamma_2$ receptors (monitoring changes in both I-GABA and FLZM potentiation of I-GABA) were as follows: control = 1 mM MTS; +FLZM = 2 mM MTS and 30 μM FLZM; +BCCM = 2 mM MTS and 1 μM BCCM; +GABA = 1 mM MTS and 4 mM GABA; +PENTO = 1 mM MTS and 500 μM PENTO. The drug concentrations used to modify α_1S106C$\beta_2\gamma_2$ receptors (monitoring changes in both I-GABA and FLZM potentiation of I-GABA) were as follows: control = 1 mM MTS; +FLZM = 1 mM MTS and 3 μM FLZM; +Ro15-1788 = 2 mM MTS and 5 μM Ro15-1788; +GABA = 1 mM MTS and 300 μM GABA.

Statistical Analysis. Data analysis was carried out using nonlinear regression analysis included in the Prism software package. Statistical analysis on MTSEA-Biotin accessibility (2 min of 2 mM MTS-Biotin pulses) and GABA and FLZM EC_{50} values was conducted using a one-way analysis of variance, followed by a post hoc Dunnett's test. Statistical analysis of MTSEA-Biotin rate calculations was performed using the False Discovery Rate Method (Benjamini and Hochberg, 1995) accessed via the University of North Texas website (http://www.unt.edu/benchmarks/archives/2002/april02/rss.htm). We thank Mary Lindstrom (Statistics Department, University of Wisconsin–Madison) and Chenlei Leng (Statistics Department, National University of Singapore) for their assistance with this method.

Results

Effects of Cysteine Mutations. Amino acid residues α_1 Asp97–Ser106 were individually mutated to cysteine (Fig. 1A) and expressed with wild-type β_2 and γ_2 subunits in *X. laevis* oocytes. In $\alpha_1\beta_2\gamma_2$ receptors, there are two α_1 subunits; thus, the introduced cysteines are located at both the α_1/γ_2 interface (BZD binding site) and the α_1/β_2 interface (non-GABA binding site) (Fig. 1B). To determine whether the introduced cysteines affected GABA$_A$ receptor function and/or expression, two-electrode voltage clamp was used to measure GABA and FLZM concentration responses (Fig. 2). With the exception of α_1T98C and α_1F100C, the mutant subunits assembled into functional $\alpha_1\beta_2\gamma_2$ receptors. For five mutant receptors, the GABA EC_{50} values were not significantly different from the wild-type receptor value (EC_{50} = 17 μM). For α_1D97C and α_1N102C containing receptors, the GABA EC_{50} values were increased 10- and 24-fold, respectively (Table 1), whereas a 4-fold decrease in GABA EC_{50} was measured for α_1S106C containing receptors. Two mutations significantly altered FLZM concentration responses. For α_1H101C- and α_1N102C-containing receptors, FLZM EC_{50} values were increased 19- and 6-fold, respectively (Table 1). There was no correlation between mutations that affected GABA EC_{50} (e.g., D97C, N102C, and S106C) and mutations that affected BZD EC_{50} (e.g., H101C, N102C) (Table 1).

Effects of MTSEA-Biotin Modification. To determine the accessibility of the introduced cysteines, wild-type and mutant receptors were exposed to MTSEA-Biotin (2 mM) for 2 min. GABA-elicited current (I-GABA) and FLZM potentiation of I-GABA were measured before and after MTSEA-Biotin exposure (Fig. 3). MTSEA-Biotin had no effect on GABA or FLZM responses in wild-type receptors. Thus, any changes measured in I-GABA or FLZM potentiation of I-GABA after MTSEA-Biotin exposure indicate that the introduced cysteine was modified. MTSEA-Biotin increased I-GABA and decreased FLZM potentiation in α_1H101C-, α_1N102C-, and α_1S106C-containing receptors, whereas in

α_1D97C-containing receptors, exposure to MTSEA-Biotin only decreased I-GABA and had no effect on FLZM potentiation. The data demonstrate that α_1D97C, α_1H101C, α_1N102C, and α_1S106C are accessible. MTSEA-Biotin had no effect on receptors containing α_1F99C, α_1G103C, α_1K104C, and α_1K105C. These residues are either inaccessible or reacted with MTSEA-Biotin, but the reactions had no functional effect. The pattern of accessibility does not predict a secondary structure such as a β-strand or α-helix (Fig. 3), and the α_1D97C-α_1S106C region is likely to be a turn or a random coil.

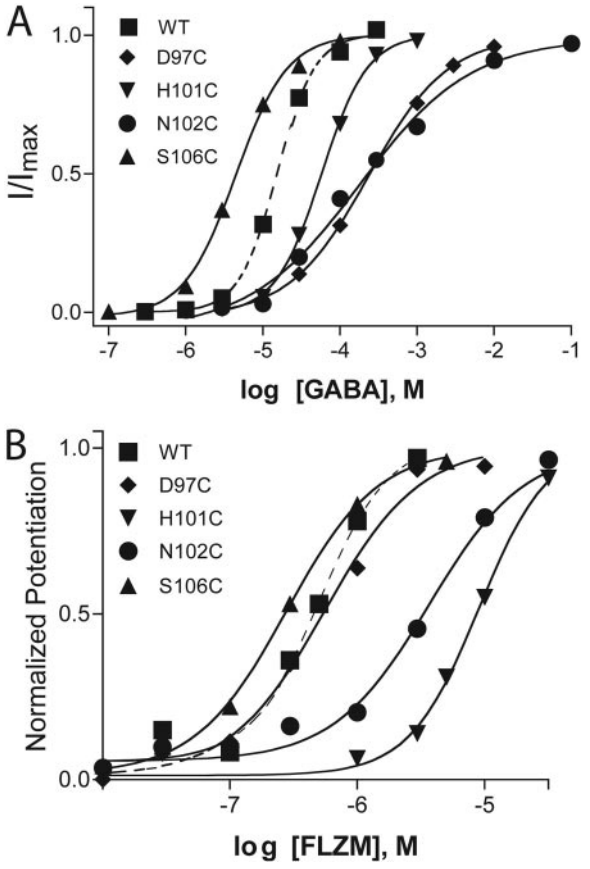

Fig. 2. Representative GABA and FLZM concentration-response curves for wild-type and mutant receptors. A, data are normalized to maximal GABA current response for each receptor. B, data are normalized to maximal FLZM potentiation of GABA (EC_{15}) current. Dashed lines are curve fits from wild-type receptors. EC_{50} values and calculated Hill coefficients are reported in Table 1.

To examine whether the increases in I-GABA and decreases in FLZM potentiation observed after MTSEA-Biotin exposure were linked, we examined the concentration of MTSEA-Biotin needed to elicit these effects in receptors containing α_1H101C. Modification of α_1H101C by MTSEA-Biotin (2 min, 2 mM) decreased FLZM potentiation of I-GABA by 97 ± 6% and increased I-GABA by 75 ± 17% (Fig. 3). In contrast, a 10 s exposure to a low concentration of MTSEA-Biotin (50 μM) almost completely abolished FLZM potentiation without altering I-GABA (Fig. 4). Subsequent treatment with a high concentration of MTSEA-Biotin (4 mM, 10 s) increased I-GABA (Fig. 4). The data suggest that the effects of MTSEA-Biotin on GABA current are not correlated with the effects on BZD modulation and are inconsistent with reciprocal regulation of GABA and BZD binding affinities.

MTSEA-Biotin Reaction Rates. The rate at which MTSEA-Biotin reacts with a cysteine side chain depends mainly on the ionization state of the thiol group and the access route to the engineered cysteine. A residue in a relatively open, aqueous environment will react faster than a residue in a relatively restrictive, nonpolar environment. As predicted from the experiments described above using a low concentration of MTSEA-Biotin, the decrease in FLZM potentiation of I-GABA, after MTSEA-Biotin modification of α_1H101C, occurred 18-fold faster than the increase in I-GABA ($k_{2\text{-}FLZM\text{-}P}$ = 2258 ± 369 M^{-1} s^{-1} versus $k_{2\text{-}IGABA}$ = 122.3 ± 10.8 M^{-1} s^{-1}) (Fig. 5). Because there are two introduced cysteines in a α_1H101C$\beta_2\gamma_2$ receptor, each rate may correspond to derivatization of an individual cysteine. For example, rapid modification of α_1H101C at the α/γ interface (BZD site) could be responsible for the decrease in BZD potentiation, whereas slow modification of α_1H101C at the α/β interface could be responsible for the increase in I-GABA. Alternatively, derivatization of the cysteine at the α/γ interface may be sufficient to decrease FLZM potentiation of I-GABA, whereas modification of both cysteines is required for the increase in I-GABA. A faster decrease in BZD potentiation versus I-GABA increase was also observed for α_1S106C$\beta_2\gamma_2$ receptors (Table 2). In α_1N102C$\beta_2\gamma_2$ receptors, MTSEA-Biotin modification decreased FLZM potentiation

TABLE 1

Summary of GABA and FLZM concentration response data for wild-type and mutant receptors

Data represent mean ± S.D. *n_H values are calculated Hill coefficients.*

Receptor	GABA EC_{50}	n_H	n	EC_{50} mut/ EC_{50} $\alpha\beta\gamma$	FLZM EC_{50}	n_H	n	EC_{50} mut/ EC_{50} $\alpha\beta\gamma$
	μM				μM			
$\alpha_1\beta_2\gamma_2$	17.4 ± 7.0	1.6 ± 0.3	4	1	0.47 ± 0.15	1.3 ± 0.3	5	1
α_1D97C$\beta_2\gamma_2$	168.8 ± 73.5	0.94 ± 0.2	4	9.7*	0.56 ± 0.12	1.1 ± 0.1	3	1.2
α_1T98C$\beta_2\gamma_2$	N.E.				N.E.			
α_1F99C$\beta_2\gamma_2$	50.6 ± 0.5	1.1 ± 0.1	3	2.9	0.43 ± 0.12	1.6 ± 0.2	3	0.91
α_1F100C$\beta_2\gamma_2$	N.E.				N.E.			
α_1H101C$\beta_2\gamma_2$	50.5 ± 26.1	1.56 ± 0.3	7	2.9	9.0 ± 0.13	1.8 ± 0.1	3	19.1*
α_1N102C$\beta_2\gamma_2$	410 ± 305	0.56 ± 0.2	7	23.6*	2.6 ± 0.95	1.0 ± 0.2	3	5.5*
α_1G103C$\beta_2\gamma_2$	10.9 ± 5.6	1.3 ± 0.3	4	0.6	0.27 ± 0.03	1.2 ± 0.4	4	0.57
α_1K104C$\beta_2\gamma_2$	13.3 ± 6.7	0.96 ± 0.2	3	0.8	0.40 ± 0.18	1.3 ± 0.5	5	0.85
α_1K105C$\beta_2\gamma_2$	23.2 ± 3.5	1.3 ± 0.1	3	1.3	0.29 ± 0.10	1.1 ± 0.2	3	0.62
α_1S106C$\beta_2\gamma_2$	4.9 ± 1.8	1.3 ± 0.1	3	0.3**	0.44 ± 0.14	1.5 ± 0.2	3	0.94

N.E., no expression.
* Statistically different from wild type ($P < 0.05$).
** Statistically different from wild type ($P < 0.001$).

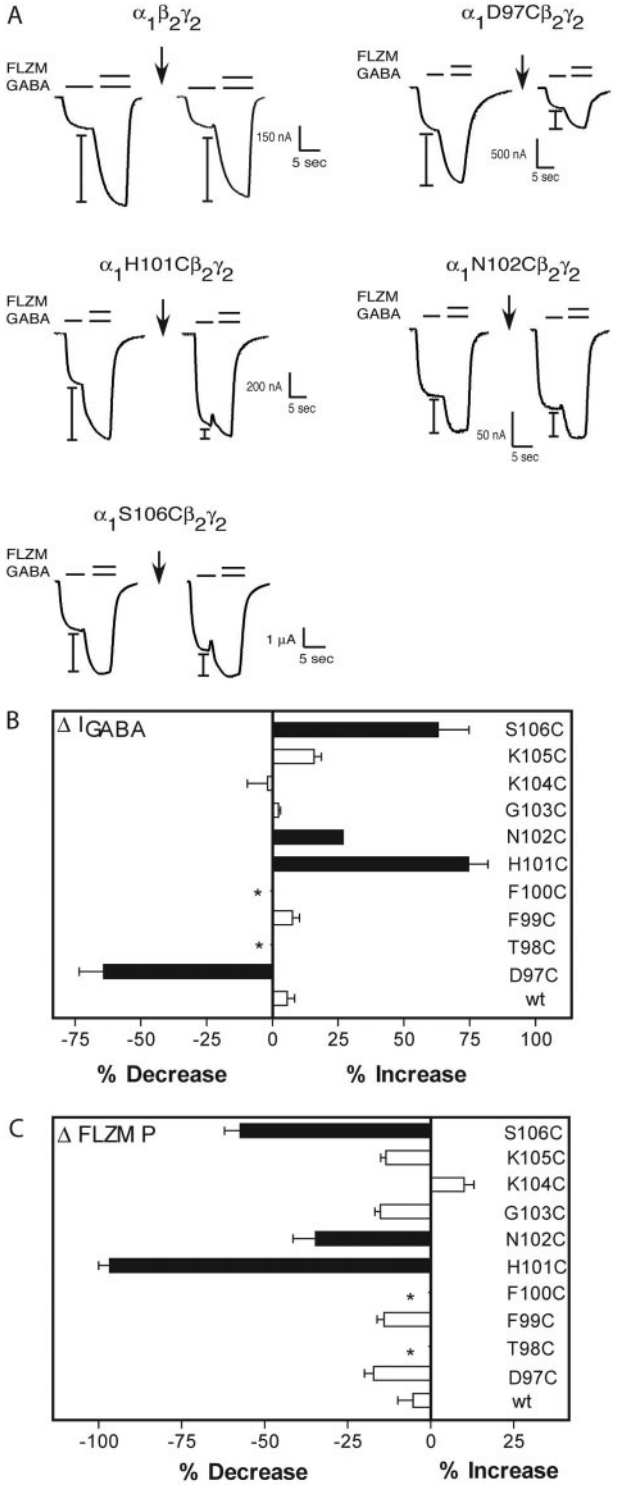

Fig. 3. Effects of MTSEA-Biotin on wild-type and mutant receptors. A, representative current traces from oocytes expressing wild-type and mutant $\alpha_1\beta_2\gamma_2$ receptors showing FLZM potentiation of I-GABA (EC_{15} GABA) before and after application of a 2 mM, 2 min pulse of MTSEA-Biotin (arrows). I-bars denote potentiation of I-GABA measured during FLZM (EC_{95}) application. B and C, bar graphs representing the percentage changes in I-GABA (ΔI-GABA) and FLZM potentiation (ΔP) after MTSEA-Biotin modification. The percentage change in I-GABA is defined as $[((\text{I-GABA-after}/\text{I-GABA-before}) - 1) \times 100]$. The percentage change in FLZM potentiation (ΔP) is defined as $[((P_{after}/P_{before}) - 1) \times 100]$. Data represent the mean ± S.D. from three or more separate experiments. Black bars indicate values that are statistically different from wild-type (wt) values ($p < 0.05$). *, no detectable functional receptor expression.

and increased I-GABA at the same rate (Table 2), suggesting that the cysteine modification is occurring at the two different interfaces with the same rates or perhaps is occurring at

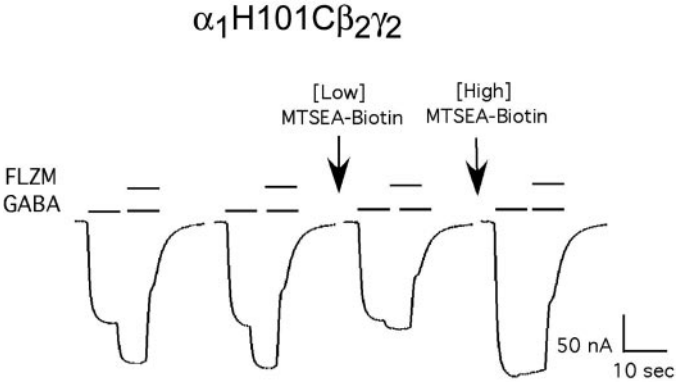

Fig. 4. Concentration dependence of MTSEA-Biotin effects on α_1H101C$\beta_2\gamma_2$ receptors. Representative GABA (EC_{15}) and GABA (EC_{15}) + FLZM (EC_{95}) current responses from a single oocyte expressing α_1H101C$\beta_2\gamma_2$ receptors. Arrows indicate 10-s exposures to a low concentration (50 μM) and then a high concentration (4 mM) of MTSEA-Biotin. FLZM potentiation of I-GABA is abolished after application of a low concentration of MTSEA-Biotin, whereas I-GABA is unchanged. Application of a subsequent high concentration of MTSEA-Biotin increases I-GABA.

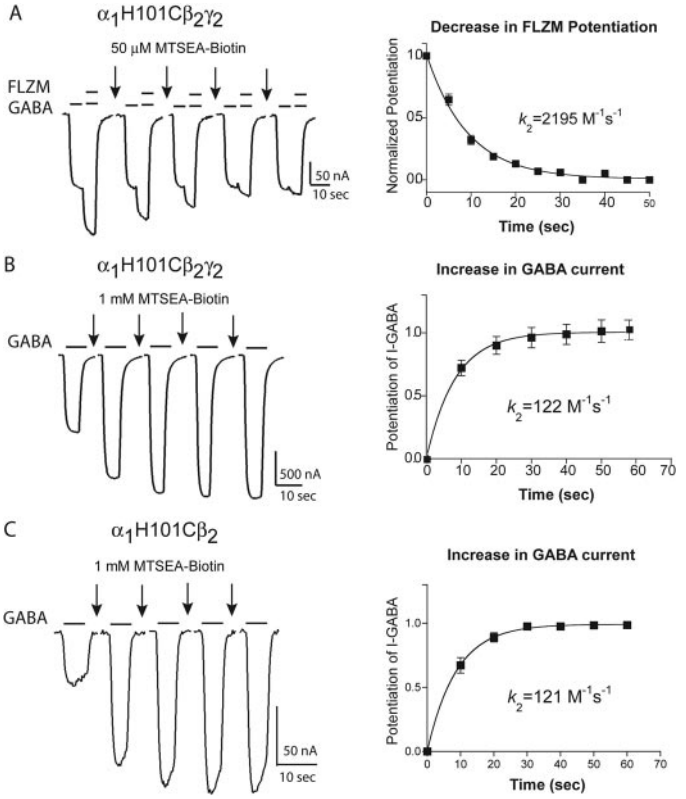

Fig. 5. Rates of MTSEA-Biotin modification of α_1H101C. Representative GABA (EC_{15}) and GABA + FLZM (EC_{95}) current responses from oocytes expressing α_1H101C$\beta_2\gamma_2$ receptors (A and B) and α_1H101Cβ_2 receptors (C) before and after 10-s applications of MTSEA-Biotin (arrows). Decreases in FLZM potentiation of I-GABA (A) and increases in I-GABA (B and C) were plotted versus cumulative MTSEA-Biotin exposure. A, data were normalized to FLZM potentiation measured before MTSEA-Biotin exposure ($t = 0$ s). B and C, data were normalized to I-GABA measured before MTSEA-Biotin exposure. The data were fit with single exponential functions and the calculated second-order rate constants (k_2) were determined as described under *Materials and Methods*. Data points represent the mean ± S.E.M. from at least five independent experiments. k_2 values are summarized in Table 2.

only one interface, and the effects on GABA current and FLZM potentiation were linked.

To examine whether modification of the introduced cysteine at the α/γ interface was required to observe the increase in I-GABA, the α_1H101C subunit was expressed with only wild-type β_2 subunits. In α_1H101Cβ_2 receptors, the mutation is present only at nonbinding site interfaces (α/β, α/α). MTSEA-Biotin treatment (2 mM, 2 min) of α_1H101Cβ_2 receptors increased I-GABA (Fig. 5C). The rate of change in I-GABA (k_2 = 121 ± 40 M^{-1} s^{-1}) (Table 2) was similar to the rate measured for α_1H101C$\beta_2\gamma_2$ receptors (k_2 = 122 ± 11 M^{-1} s^{-1}) (Table 2) and suggests that modification of the α_1H101C at the α/β interface is responsible for the increase in I-GABA.

To examine whether modification of α_1H101C at the α/γ interface caused the decrease in FLZM potentiation measured, we examined the ability of BZD-site ligands (FLZM and Ro15-1788) to slow covalent modification of α_1H101C (Fig. 6). We reasoned that if the decrease in FLZM potentiation was caused by modification of α_1H101C at the α/γ interface, then the presence of BZD binding-site ligands should sterically block the site and slow the decrease in FLZM potentiation. Both FLZM and Ro15-1788 significantly slowed the rate of decrease in BZD potentiation caused by MTSEA-Biotin modification (3- and 37-fold, respectively; Table 3). FLZM had no effect on the rate of increase in I-GABA, whereas Ro15-1788 significantly increased the rate by 2-fold (Table 3). Taken together, these data support the hypothesis that rapid modification of α_1H101C at the α/γ interface (BZD binding site) is responsible for the decrease in FLZM potentiation and slow modification at the α/β interface (nonbinding site) is responsible for the increase in GABA-mediated current.

Effects of GABA, Muscimol, SR-95531, and Pentobarbital on MTSEA-Biotin Reaction Rates. Because we could independently detect changes at the α/γ (BZD site) and α/β subunit interfaces by monitoring the decrease in FLZM potentiation versus the increase in I-GABA, respectively, we used the technique to determine whether the presence of GABA altered the structure of the BZD binding site near α_1H101C. By examining and comparing rates of modification of introduced cysteines in the presence of BZDs, SR-95531, GABA, and pentobarbital, one can begin to tease apart movements induced by each of these ligands and elucidate differences between the conformational states stabilized by their binding. For example, because GABA and SR-95531 bind to the same site but GABA promotes channel opening/desensitization, whereas the competitive antagonist SR-99531 does not, the simplest interpretation of differences in rates is that the rate in the presence of GABA reflects motions specifically induced by GABA binding and gating the channel (stabilization of open/desensitized states), whereas the rate in the presence of SR-95531 reflects motions specifically induced by SR-95531 binding and stabilization of a closed state.

GABA (EC_{95}) significantly increased (4-fold) the rate at which MTSEA-Biotin modifies α_1H101C at the α/γ interface (detected by measuring the decrease in FLZM potentiation), suggesting that GABA binding and/or channel opening/desensitization caused movements within the BZD binding site (Fig. 7, Table 3). Muscimol (a $GABA_AR$ agonist) had a similar effect (8577 ± 994 M^{-1} s^{-1}, n = 3), whereas SR-95531 (a $GABA_AR$ antagonist) caused a significant decrease in the MTSEA-Biotin reaction rate (1439 ± 81 M^{-1} s^{-1}, $p < 0.05$, n = 3). To determine whether the changes observed in the BZD binding site in the presence of GABA and muscimol were due to a global conformational change associated with

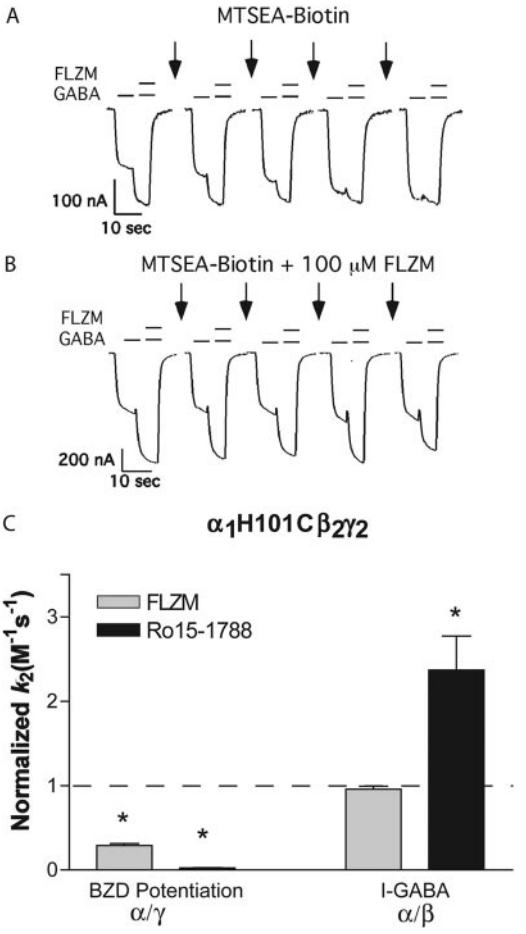

Fig. 6. The effect of FLZM and Ro15-1788 on the rate of MTSEA-Biotin modification of α_1H101C. A and B, GABA (EC_{15}) and GABA + FLZM (EC_{95}) current responses from oocytes expressing α_1H101C$\beta_2\gamma_2$ receptors before and after applications of 50 μM MTSEA-Biotin alone (A) or in the presence of a saturating concentration of FLZM (B). C, MTSEA-Biotin k_2 values were measured in the presence of FLZM (BZD agonist) and Ro 15−1788 (BZD antagonist) and normalized to values measured in the absence of these ligands (control, dashed line). Rate constants for the decrease in BZD potentiation (α/γ interface) and the increase in I-GABA (α/β interface) were measured. BZD-site ligands significantly slowed the rate of decrease in BZD potentiation caused by MTSEA-Biotin modification but did not slow the rate of increase in I-GABA. *, values significantly different from control ($p < 0.05$). k_2 values are summarized in Table 3.

TABLE 2

Second-order rate constants (k_2) for decreases in BZD potentiation and changes in I-GABA after MTSEA-biotin modification of mutant receptors

The concentrations of MTSEA-Biotin used were variable depending on the mutant and are listed under *Materials and Methods*. Values are mean ± S.D.

Receptor	BZD Potentiation k_2 (M^{-1} s^{-1})	n	I-GABA k_2 (M^{-1} s^{-1})	n
α_1D97C$\beta_2\gamma_2$			20.5 ± 5.7	6
α_1H101C$\beta_2\gamma_2$	2194.6 ± 354.1	6	122.3 ± 10.8*	5
α_1N102C$\beta_2\gamma_2$	46.7 ± 5.5	7	52.9 ± 22.1	8
α_1S106C$\beta_2\gamma_2$	28.9 ± 8.2	6	11.3 ± 3.9*	7
α_1H101Cβ_2			121.4 ± 40.4	5

* The decrease in BZD potentiation was significantly faster than the increase in I-GABA ($P < 0.05$).

channel gating, we examined the rate at which MTSEA-Biotin modified α_1H101C in the presence of pentobarbital at a concentration that directly gates the channel. Pentobarbital had no effect on the rate of MTSEA-Biotin modification in the BZD binding site (Fig. 7) even though it elicited approximately the same amount of current as EC_{max} GABA (84.0 ± 10.0%; data not shown). Thus, although GABA and pentobarbital both caused similar amounts of channel activation, a change in the structure of the BZD binding site near α_1H101C was only detectable in the presence of ligands that occupy the GABA binding site. Similar results were seen in α_1N102C$\beta_2\gamma_2$ receptors (Table 3). GABA had no effect on the rates of modification of α_1D97C$\beta_2\gamma_2$ or α_1S106C$\beta_2\gamma_2$ receptors (Table 3).

It is noteworthy that the presence of GABA did not alter the rate MTSEA-Biotin modified α_1H101C or α_1N102C located at the α/β interface (i.e., no change in the slow reaction rate associated with the increase in I-GABA; Fig. 7, Table 3) whereas pentobarbital significantly increased the rate of modification of α_1N102C located at the α/β interface.

Effects of BZD Ligands on MTSEA-Biotin Reaction Rates. The rates at which MTSEA-Biotin modifies α_1D97C, α_1N102C, and α_1S106C are significantly slower than for α_1H101C, suggesting that these residues are in a less accessible/hydrophilic environment than α_1H101C (Table 2). To examine whether these residues line the BZD binding pocket of the receptor or change environment in response to BZD binding, we tested the effect of different BZD ligands on the rate at which MTSEA-Biotin modifies the introduced cysteines. A BZD could slow the rate of reaction at a substituted cysteine because it sterically blocks (protects) the residue from the MTS reagent, suggesting that the residue is facing into the BZD binding site. Alternatively, the reaction rate could be reduced by ligand-induced allosteric changes in the protein structure that result in the cysteine's being in a less accessible environment. We use the following criteria to identify a residue that lines the core of the BZD binding pocket: 1) when mutated to cysteine, the residue is accessible to covalent modification by MTSEA-Biotin, 2) its modification decreases BZD modulation of GABA current, and 3) its rate of modification by MTSEA-Biotin *decreases* in the presence of at least two different BZD ligands that have different functional properties (e.g., BZD agonist versus BZD antagonist, BZD agonist versus BZD inverse-agonist), which cause different local conformational rearrangements within the receptor. Because mutations can cause changes in BZD efficacies (Mihic et al., 1994; Dunn et al., 1999; Crestani et al., 2002; Kelly et al., 2002), for each mutation, we checked the efficacy of the BZD ligands being used in our rate experiments. This was necessary to ensure that we were testing and comparing the effects of BZD ligands that had different efficacies.

Both FLZM (BZD agonist) and Ro15-1788 (BZD antagonist) slowed MTSEA-modification of α_1H101C (Fig. 6, Table 3) at the α/γ interface (monitoring BZD potentiation), indicating that α_1H101C faces into the BZD binding pocket. This result is consistent with results from photolabeling, mutagenesis, and modeling studies (Duncalfe et al., 1996; Dunn et al., 1999; Sigel, 2002). At α_1N102C$\beta_2\gamma_2$ receptors, BCCM (BZD antagonist with this mutation) but not FLZM (BZD agonist) slowed the rate of MTSEA-Biotin reaction at the α/γ interface (Table 3), suggesting that α_1N102C probably does not face directly into the BZD binding pocket. At the α/γ interface, FLZM (BZD agonist) increased MTSEA-Biotin modification of α_1S106C, whereas Ro15-1788 (BZD antagonist) slowed its modification (Table 3), suggesting that α_1S106C does not line the BZD binding pocket and that this residue may be a reporter for different structural changes that occur when a BZD agonist versus antagonist binds.

Modification of α_1D97C by MTSEA-Biotin had no effect on FLZM potentiation of I-GABA but decreased I-GABA (Fig. 3). For this mutation, it is unclear whether modification is occurring at both the α_1/γ_2 and α_1/β_2 interfaces. Nevertheless, if α_1D97C were facing into the core of the BZD binding site, one would expect a decrease in FLZM potentiation when the residue was derivatized as a result of MTSEA-Biotin occlusion of the binding site. Both FLZM (BZD agonist) and BCCM (BZD antagonist) slowed the rate at which MTSEA-Biotin modification decreased I-GABA (Table 3). We speculate that occupation of the BZD binding site by either FLZM or BCCM is likely to induce structural rearrangements in the receptor that allosterically decrease α_1D97C accessibility.

Discussion

GABA-A receptor function is modulated by a variety of clinically important drugs, including BZDs, barbiturates, and neurosteroids. Structural mechanisms by which these allosteric drug modulators exert their distinct actions are

TABLE 3

Second-order rate constants for MTSEA-Biotin derivatization of mutant receptors in the absence and presence of FLZM, Ro15–1788, βCCM, GABA, and PENTO

Data are presented as molar^{-1} seconds^{-1}. Data represent mean ± S.D.

	Control k_2	n	FLZM k_2	n	Ro15–1788 k_2	n	BCCM k_2	n	GABA k_2	n	PENTO k_2	n
FLZM P												
α_1H101C$\beta_2\gamma_2$	2194.6 ± 354.1	6	678.3 ± 145.8*	4	59.0 ± 18.2*	3	N.D.		9047.5 ± 1494.0*	4	2299.0 ± 457.6	4
α_1N102C$\beta_2\gamma_2$	46.7 ± 5.5	7	30.9 ± 3.0	3	—†		16.9 ± 3.7*	3	91.2 ± 24.7*	3	54.5 ± 14.9	3
α_1S106C$\beta_2\gamma_2$	28.9 ± 8.2	6	45.6 ± 7.5*	3	11.9 ± 3.1*	3	N.D.		20.0 ± 5.4	3	N.D.	
I-GABA												
α_1D97C$\beta_2\gamma_2$	20.5 ± 5.7	6	9.2 ± 3.3*	3	—†		Block		20.6 ± 5.2	3	N.D.	
α_1H101C$\beta_2\gamma_2$	122.3 ± 10.8	5	117.2 ± 5.0	4	289.8 ± 136.8*	5	N.D.		154.4 ± 42.6	5	N.D.	
α_1N102C$\beta_2\gamma_2$	52.9 ± 22.1	8	32.1 ± 11.7	3	—†		11.7 ± 1.0*	3	81.2 ± 9.2	3	124.2 ± 47.7*	4
α_1S106C$\beta_2\gamma_2$	11.3 ± 3.9	7	12.0 ± 4.0	3	7.0 ± 1.0	4	N.D.		9.7 ± 5.3	3	N.D.	
α_1H101Cβ_2	121.4 ± 40.4	5	101.4 ± 27.7	3	145.8 ± 19.3	3	N.D.		166.5 ± 34.4	4	N.D.	

"Block" indicates that BCCM slowed the rate of modification of α_1D97C to the extent that a rate could not be accurately determined using the available MTSEA-Biotin concentrations. N.D., not determined.

* Significantly different from control rates ($P < 0.05$).

† Rates were not measured because Ro15-1788 potentiated I-GABA.

unclear. In this study, we developed an assay that allowed us to separately monitor the conformational state of each α_1 subunit (α/γ interface, α/β interface) in the absence (resting state) and presence of orthosteric agonists and antagonists, BZD modulators, and pentobarbital. Several lines of evidence can be used to make the argument that the observed decreases in BZD potentiation and increases in I-GABA after MTS modification of α_1H101C-containing receptors result from reaction at the BZD (α/γ) and nonbinding (α/β) interfaces, respectively. At α_1H101C$\beta_2\gamma_2$ receptors, the MTS-induced decrease in BZD potentiation occurred 18-fold faster than the I-GABA increase. As the rate of reaction at an engineered cysteine reflects the environment surrounding it, reactions at two different α_1His101 mutant cysteines are probably responsible for the disparate rates. Second, BZD site agonists protected against the decrease of BZD potentiation but not the I-GABA increase. Finally, the presence of the γ subunit was not necessary for the increase in I-GABA because removal of the BZD-site by expressing α_1H101C with only a wild-type β_2 subunit resulted in an I-GABA increase after MTS application.

When GABA is present (open/desensitized states), α_1H101C and α_1N102C at the BZD binding site (α/γ interface) are more accessible to modification by MTSEA-Biotin than when the receptor is in the unliganded resting state. This result is in agreement with a study by Berezhnoy et al. (2005), who found that modification of H101C by a cysteine-reactive BZD was increased in the presence of GABA. Agonist occupation of the GABA binding site probably induces a closure of the GABA binding site cavity located at the β/α interface (Jones et al., 2001; Wagner and Czajkowski, 2001; Amiri et al., 2007). We speculate that the closure of the GABA binding site upon ligand occupation leads to a reciprocal opening of the BZD binding site at the α/γ interface, which increases the rate of α_1H101C modification. This idea is consistent with radioligand binding studies that have shown that GABA binding site agonists increase the binding of BZDs (Tallman et al., 1978; Karobath and Sperk, 1979).

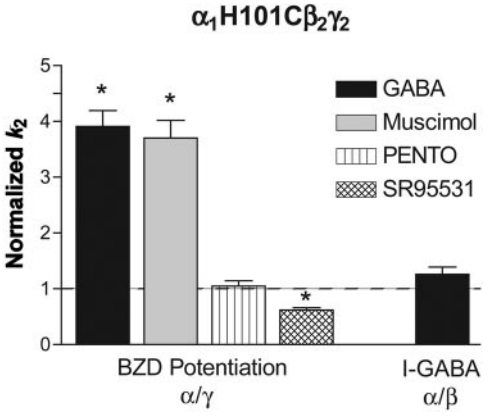

Fig. 7. The effects of GABA, muscimol, pentobarbital, and SR-95531 on MTSEA-Biotin second-order rate constants. Second-order rate constants for MTSEA-Biotin modification of α_1H101C in the absence (control) and presence of GABA (EC_{95}), muscimol (EC_{95}), pentobarbital (PENTO, 500 μM), and SR-95531 (IC_{95}) were measured as described under *Materials and Methods*. Rate constants for both the decrease in BZD potentiation (α/γ) and the increase in I-GABA (α/β) were measured and normalized to the MTSEA-Biotin reaction rates measured in the absence of these ligands (control, dashed line). Data represent mean ± S.D. from at least three experiments. *, significantly different from control ($p < 0.05$). k_2 values are shown in Table 3.

The GABA-site antagonist SR-95531 makes α_1H101C at the BZD-site less accessible to MTS-Biotin modification, indicating that occupation of the GABA binding site without channel activation is sufficient to modulate the BZD binding site and that binding of GABA-site antagonists and agonists induce distinct conformational rearrangements in the BZD site near α_1H101C. The results are consistent with the idea that antagonist binding to the GABA binding site induces a movement in the GABA binding site interface that causes a closure of the BZD binding site cavity. Moreover, these data demonstrate that binding of a competitive antagonist to the GABA binding site (β/α interface) induces movements in the receptor that can extend over considerable distances to the α/γ (BZD-site) interface.

Our data also demonstrate that whereas GABA increases the accessibility of α_1H101C located at the BZD binding site, it has no affect at the α/β interface. Although each α_1 subunit contributes to a GABA binding site, our data suggest that GABA may cause asymmetrical structural movements in the α_1 subunits, depending upon their positions in the pentamer. Recent findings support the theory of asymmetrical gating movements in cys-loop receptors (Unwin et al., 2002; Miyazawa et al., 2003; Shen et al., 2003). Shan and colleagues demonstrate that the α and β subunits in a heteromeric glycine receptor adopt structurally distinct conformations during receptor activation (Shan et al., 2003). We cannot, however, rule out the possibility that GABA causes movements at each subunit interface and that the increase in the accessibility of α_1H101C can only be detected at the BZD-site as a result of differences in the physicochemical environments of the two different subunit interfaces (α/γ, α/β).

At low concentrations, pentobarbital allosterically modulates the GABA-A receptor and increases the mean channel open time when GABA is bound (Twyman et al., 1989; Steinbach and Akk, 2001). At high concentrations, pentobarbital can gate the channel directly (Nicoll and Wojtowicz, 1980). We hypothesized that a directly activating concentration of pentobarbital, which stabilizes an open-channel state that is similar to the GABA-activated state (Jackson et al., 1982; Rho et al., 1996; Steinbach and Akk, 2001), would result in movements in the BZD binding site similar to those induced by GABA. To our surprise, 500 μM pentobarbital did not induce movements in the BZD binding site near residues α_1H101C or α_1N102C, indicating that the BZD site responds with distinct conformation changes to channel activation by different ligands. Moreover, the data suggest that GABA binding site occupation and not global receptor transitions associated with channel gating regulates BZD binding site movement near α_1His101. Our data are not consistent with a recent study that reported that pentobarbital increased the rate of modification of α_1H101C by a sulfhydryl-reactive BZD agonist (Berezhnoy et al., 2005). Because their sulfhydryl-reactive BZD has an affinity for the BZD binding site, interpreting changes in its rates of modification of H101C are complicated. The rate also depends on its affinity for the BZD site as well as ionization of the cysteine, and its affinity will change in the presence of different ligands. Thus, it is difficult to determine whether the apparent increase in rate of H101C modification in the presence of pentobarbital was due to an increased affinity or to an increase in rate of covalent reaction. Because it is known that pentobarbital increases

the affinity of BZDs (Leeb-Lundberg et al., 1990), the increase in rate would be expected and may reflect a change in the overall structure of the BZD binding site. Therefore, it is not surprising that the pentobarbital results from Berezhnoy et al. (2005) are not in agreement with our data. It is possible that pentobarbital induces movements in regions of the BZD site not monitored in our study. The changes in rates reported in our article reflect changes in the *local environment* near the engineered cysteine. It is noteworthy that 500 μM pentobarbital induced structural rearrangements near α_1N102C at the α/β interface, suggesting that the α_1 subunits at different interfaces are differently modulated by pentobarbital activation of the channel, which again support the idea of asymmetrical gating movements.

Both FLZM and Ro15-1788 slowed MTSEA-modification of α_1H101C (Fig. 6, Table 3) at the α/γ interface. However, FLZM and Ro15-1788 differentially modulate accessibility of α_1H101C at the α/β interface. Although FLZM had no effect on α_1H101C accessibility, Ro15-1788 significantly increased its rate of modification, indicating that FLZM and Ro15-1788 do not induce identical movements and suggesting that the actions of different BZDs are mediated by promoting different rearrangements in the receptor. Moreover, the data indicate that BZD binding can evoke structural movements that extend from the BZD binding site not only to the GABA binding site (Kloda and Czajkowski, 2007) but also to a nonbinding site interface (α/β).

Our data suggest that α_1N102 does not face into the BZD binding pocket because FLZM did not significantly slow the rate of MTSEA-Biotin reaction at the α/γ interface. However, BCCM, which acts as a BZD antagonist at α_1N102C$\beta_2\gamma_2$ receptors does slow the rate of MTSEA-Biotin modification suggesting that α_1N102C is a reporter for different structural changes triggered by BZD agonist versus antagonist binding. In a similar fashion, α_1S106C may report structural changes associated with Ro15-1788 versus FLZM agonist binding. Our data, however, are not consistent with conclusions reached by Tan et al. (2007), who suggest that α_1N102 faces into the BZD-site based on the ability of a cysteine-reactive derivative of Ro15-4513 to covalently react with α_1N102C. It is possible, given the different structures of FLZM, BCCM, and Ro15-4513, that Ro15-4513 and BCCM occupy the site differently than FLZM and that α_1N102 forms part of a subsite within the BZD binding pocket that is important for BCCM and Ro15-4513 binding.

In summary, we have monitored ligand-induced movements in the GABA-A receptor at defined subunit interfaces. We demonstrate that GABA and muscimol trigger movements in the BZD binding site near α_1His101 that are consistent with an opening up of the BZD binding site, whereas the competitive antagonist SR-95531 stabilizes a receptor conformation that probably induces BZD binding site closure. Pentobarbital produces no conformational changes in this region of the BZD binding site. Thus, channel opening does not necessarily propagate back to the BZD binding site. We hypothesize that the GABA and BZD binding sites, which are both localized in the extracellular domain of the receptor, are physically linked such that occupation of the GABA binding site alone is sufficient to cause movements in the BZD binding site and that this linkage is part of the mechanism by which the two sites are allosterically coupled.

References

Amiri S, Sansom MS, and Biggin PC (2007) Molecular dynamics studies of AChBP with nicotine and carbamylcholine: the role of water in the binding pocket. *Protein Eng Des Sel* **20:**353–359.

Benjamini Y and Hochberg Y (1995) Controlling the false discovery rate: a practical and powerful approach to multiple testing. *J R Statist Soc Ser B* **57:**289–300.

Berezhnoy D, Baur R, Gonthier A, Foucaud B, Goeldner M, and Sigel E (2005) Conformational changes at benzodiazepine binding sites of GABA$_A$ receptors detected with a novel technique. *J Neurochem* **92:**859–866.

Boileau AJ and Czajkowski C (1999) Identification of transduction elements for benzodiazepine modulation of the GABA$_A$ receptor: three residues are required for allosteric coupling. *J Neurosci* **19:**10213–10220.

Boileau AJ, Evers AR, Davis AF, and Czajkowski C (1999) Mapping the agonist binding site of the GABA$_A$ receptor: evidence for a beta-strand. *J Neurosci* **19:** 4847–4854.

Boileau AJ, Kucken AM, Evers AR, and Czajkowski C (1998) Molecular dissection of benzodiazepine binding and allosteric coupling using chimeric γ-aminobutyric acid$_A$ receptor subunits. *Mol Pharmacol* **53:**295–303.

Boileau AJ, Newell JG, and Czajkowski C (2002) GABA$_A$ receptor β2 Tyr97 and Leu99 line the GABA-binding site. Insights into mechanisms of agonist and antagonist actions. *J Biol Chem* **277:**2931–2937.

Braestrup C, Schmiechen R, Neef G, Nielsen M, and Petersen EN (1982) Interaction of convulsive ligands with benzodiazepine receptors. *Science* **216:**1241–1243.

Choi DW, Farb DH, and Fischbach GD (1981) Chlordiazepoxide selectively potentiates GABA conductance of spinal cord and sensory neurons in cell culture. *J Neurophysiol* **45:**621–631.

Crestani F, Assandri R, Tauber M, Martin JR, and Rudolph U (2002) Contribution of the alpha1-GABA$_A$ receptor subtype to the pharmacological actions of benzodiazepine site inverse agonists. *Neuropharmacology* **43:**679–684.

Doble A and Martin IL (1996) *The GABAA/Benzodiazepine Receptor As a Target for Psychoactive Drugs.* R.G. Landes, Austin.

Duncalfe LL, Carpenter MR, Smillie LB, Martin IL, and Dunn SM (1996) The major site of photoaffinity labeling of the γ-aminobutyric acid type A receptor by [^{3}H]flunitrazepam is histidine 102 of the α subunit. *J Biol Chem* **271:**9209–9214.

Dunn SM, Davies M, Muntoni AL, and Lambert JJ (1999) Mutagenesis of the rat alpha1 subunit of the γ-aminobutyric acid$_A$ receptor reveals the importance of residue 101 in determining the allosteric effects of benzodiazepine site ligands. *Mol Pharmacol* **56:**768–774.

Hattori K, Oomura Y, and Akaike N (1986) Diazepam action on gamma-aminobutyric acid-activated chloride currents in internally perfused frog sensory neurons. *Cell Mol Neurobiol* **6:**307–323.

Hevers W and Luddens H (1998) The diversity of GABA$_A$ receptors. Pharmacological and electrophysiological properties of GABA$_A$ channel subtypes. *Mol Neurobiol* **18:**35–86.

Jackson MB, Lecar H, Mathers DA, and Barker JL (1982) Single channel currents activated by gamma-aminobutyric acid, muscimol, and (-)-pentobarbital in cultured mouse spinal neurons. *J Neurosci* **2:**889–894.

Jones MV, Jonas P, Sahara Y, and Westbrook GL (2001) Microscopic kinetics and energetics distinguish GABA$_A$ receptor agonists from antagonists. *Biophys J* **81:** 2660–2670.

Karobath M and Sperk G (1979) Stimulation of benzodiazepine receptor binding by gamma-aminobutyric acid. *Proc Natl Acad Sci U S A* **76:**1004–1006.

Kelly MD, Smith A, Banks G, Wingrove P, Whiting PW, Atack J, Seabrook GR, and Maubach KA (2002) Role of the histidine residue at position 105 in the human alpha 5 containing GABA$_A$ receptor on the affinity and efficacy of benzodiazepine site ligands. *Br J Pharmacol* **135:**248–256.

Kloda JH and Czajkowski C (2007) Agonist-, antagonist-, and benzodiazepine-induced structural changes in the alpha1 Met113-Leu132 region of the GABA$_A$ receptor. *Mol Pharmacol* **71:**483–493.

Kucken AM, Wagner DA, Ward PR, Teissere JA, Boileau AJ, and Czajkowski C (2000) Identification of benzodiazepine binding site residues in the γ2 subunit of the γ-aminobutyric acid(A) receptor. *Mol Pharmacol* **57:**932–939.

Leeb-Lundberg F, Snowman A, and Olsen RW (1980) Barbiturate receptor sites are coupled to benzodiazepine receptors. *Proc Natl Acad Sci U S A* **77:**7468–7472.

Liman ER, Tytgat J, and Hess P (1992) Subunit stoichiometry of a mammalian K^+ channel determined by construction of multimeric cDNAs. *Neuron* **9:**861–871.

Macdonald R and Barker JL (1978) Benzodiazepines specifically modulate GABA-mediated postsynaptic inhibition in cultured mammalian neurones. *Nature* **271:** 563–564.

Macdonald RL, Twyman RE, Ryan-Jastrow T, and Angelotti TP (1992) Regulation of GABA$_A$ receptor channels by anticonvulsant and convulsant drugs and by phosphorylation. *Epilepsy Res Suppl* **9:**265–277.

McKernan RM, and Whiting PJ (1996) Which GABA$_A$-receptor subtypes really occur in the brain? *Trends Neurosci* **19:**139–143.

Mihic SJ, Whiting PJ, Klein RL, Wafford KA, and Harris RA (1994) A single amino acid of the human gamma-aminobutyric acid type A receptor gamma 2 subunit determines benzodiazepine efficacy. *J Biol Chem* **269:**32768–32773.

Miyazawa A, Fujiyoshi Y, and Unwin N (2003) Structure and gating mechanism of the acetylcholine receptor pore. *Nature* **423:**949–955.

Nicoll RA and Wojtowicz JM (1980) The effects of pentobarbital and related compounds on frog motoneurons. *Brain Res* **191:**225–237.

Oakley NR and Jones BJ (1980) The proconvulsant and diazepam-reversing effects of ethyl-beta-carboline-3-carboxylate. *Eur J Pharmacol* **68:**381–382.

Olsen RW and Snowman AM (1982) Chloride-dependent enhancement by barbiturates of gamma-aminobutyric acid receptor binding. *J Neurosci* **2:**1812–1823.

Ortells MO and Lunt GG (1995) Evolutionary history of the ligand-gated ion-channel superfamily of receptors *Trends Neurosci* **18:**121–127.

Rho JM, Donevan SD, and Rogawski MA (1996) Direct activation of $GABA_A$ receptors by barbiturates in cultured rat hippocampal neurons. *J Physiol* **497:**509–522.
Robertson GA, Warmke JM, and Ganetzky B (1996) Potassium currents expressed from *Drosophila* and mouse eag cDNAs in *Xenopus* oocytes. *Neuropharmacology* **35:**841–850.
Rogers CJ, Twyman RE, and Macdonald RL (1994) Benzodiazepine and beta-carboline regulation of single $GABA_A$ receptor channels of mouse spinal neurones in culture. *J Physiol* **475:**69–82.
Rudolph U, Crestani F, and Mohler H (2001) $GABA_A$ receptor subtypes: dissecting their pharmacological functions. *Trends Pharmacol Sci* **22:**188–194.
Rudolph U and Mohler H (2004) Analysis of $GABA_A$ receptor function and dissection of the pharmacology of benzodiazepines and general anesthetics through mouse genetics. *Annu Rev Pharmacol Toxicol* **44:**475–498.
Shan Q, Nevin ST, Haddrill JL, and Lynch JW (2003) Asymmetric contribution of alpha and beta subunits to the activation of alphabeta heteromeric glycine receptors. *J Neurochem* **86:**498–507.
Shen XM, Ohno K, Tsujino A, Brengman JM, Gingold M, Sine SM, and Engel AG (2003) Mutation causing severe myasthenia reveals functional asymmetry of AChR signature cystine loops in agonist binding and gating. *J Clin Invest* **111:**497–505.
Sieghart W (2006) Structure, pharmacology, and function of $GABA_A$ receptor subtypes. *Adv Pharmacol* **54:**231–263.
Sigel E (2002) Mapping of the benzodiazepine recognition site on $GABA_A$ receptors. *Curr Top Med Chem* **2:**833–839.
Steinbach JH and Akk G (2001) Modulation of $GABA_A$ receptor channel gating by pentobarbital. *J Physiol* **537:**715–733.
Sullivan DA and Cohen JB (2000) Mapping the agonist binding site of the nicotinic acetylcholine receptor. Orientation requirements for activation by covalent agonist. *J Biol Chem* **275:**12651–12660.
Tallman JF, Thomas JW, and Gallager DW (1978) GABAergic modulation of benzodiazepine binding site sensitivity. *Nature* **274:**383–385.
Tan KR, Baur R, Gonthier A, Goeldner M, and Sigel E (2007) Two neighboring residues of loop A of the alpha(1) subunit point towards the benzodiazepine binding site of $GABA_A$ receptors. *FEBS Lett* **581:**4718–4722.
Twyman RE, Rogers CJ, and Macdonald RL (1989) Pentobarbital and picrotoxin have reciprocal actions on single $GABA_A$ receptor channels. *Neurosci Lett* **96:**89–95.
Unwin N, Miyazawa A, Li J, and Fujiyoshi Y (2002) Activation of the nicotinic acetylcholine receptor involves a switch in conformation of the alpha subunits. *J Mol Biol* **319:**1165–1176.
Wagner DA and Czajkowski C (2001) Structure and dynamics of the GABA binding pocket: A narrowing cleft that constricts during activation. *J Neurosci* **21:**67–74.

Address correspondence to: Dr. Cynthia Czajkowski, Dept. of Physiology, University of Wisconsin, 601 Science Drive, Madison, WI 53711. E-mail: czajkowski@physiology.wisc.edu